Effects of intraseasonal variation of summer monsoon rainfall on stable isotope and growth rate of a stalagmite from northwestern Thailand

Binggui Cai,[1,2] Nathsuda Pumijumnong,[3] Ming Tan,[1] Chotika Muangsong,[3] Xinggong Kong,[4] Xiuyang Jiang,[4] and Sulan Nan[5]

Received 14 October 2009; revised 12 July 2010; accepted 2 August 2010; published 4 November 2010.

[1] An annually laminated stalagmite from Namjang cave (19°40′30″N, 98°12′12″E), northwestern Thailand, has been analyzed to investigate the annual resolution climate signal persevered within its oxygen isotopic composition (δ^{18}O) and growth rate parameters. The cave site is under the influence of Asian monsoon, and local rainfall shows noticeable variations through the monsoon season. Both δ^{18}O and growth rate records, covering the last 105 years, exhibit persistent decadal-scale variability and can be compared with local instrumental data. Low δ^{18}O values coincide with high growth rates in the specimen and correspond to higher relative amounts of rainfall in later monsoon season (August–October; hereinafter referred to as ASO rainfall) versus rainfall in early monsoon season (May–July; hereinafter referred to as MJJ rainfall). The strong correlation between the δ^{18}O value and the 5 year averaged ratio of ASO to MJJ rainfall ($r = -0.50$, $p < 0.001$) indicates a significant imprint of intraseasonal variation of monsoonal rainfall on stalagmite δ^{18}O. The close resemblance between the speleothem δ^{18}O record and Western Pacific Warm Pool (WPWP) sea surface temperature (SST) implies that the WPWP may play an important role on the decadal variability of later monsoon rainfall in this region. Unique in its annual chronology, high-resolution δ^{18}O, and direct comparison with instrumental data, our record shows for the first time that the climate in northwestern Thailand has undergone decadal-scale variability and speleothem δ^{18}O is a robust proxy for regional monsoon intensity.

Citation: Cai, B., N. Pumijumnong, M. Tan, C. Muangsong, X. Kong, X. Jiang, and S. Nan (2010), Effects of intraseasonal variation of summer monsoon rainfall on stable isotope and growth rate of a stalagmite from northwestern Thailand, *J. Geophys. Res.*, *115*, D21104, doi:10.1029/2009JD013378.

1. Introduction

[2] High-resolution climate records are in a desperate need for heavily populated Southeast Asia, where monsoon-related droughts and floods have enormous economical and societal impacts [*Intergovernmental Panel on Climate Change* (*IPCC*), 2007]. With potentials for absolute chronological control and high-resolution sampling, speleothems from monsoonal regions have been extensively studied and high-quality climate records are successfully produced [e.g., *Burns et al.*, 2001; *Cai et al.*, 2008; *Fleitmann et al.*, 2007; *Hu et al.*, 2008; *Tan et al.*, 2003; *Wang et al.*, 2008; *Yuan et al.*, 2004; *Zhang et al.*, 2008]. However, in some cases interpretation of speleothem climate proxies can be ambiguous. For instance, oxygen isotopic composition (δ^{18}O) in speleothem could represent local surface temperature, precipitation amount, rainfall source, or moisture trajectory, largely depending on the climatic circumstances of cave sites [*Lachniet*, 2009; *McDermott*, 2004]. Proxy signals in speleothems could even be masked by the hydrological process in epikarst and calcite crystallization process in caves [*Fairchild et al.*, 2006]. In monsoonal regions, stalagmite δ^{18}O variation is typically linked to fluctuation of rainfall amount [e.g., *Burns et al.*, 2001, 2002]. This paradigm was recently challenged that speleothem δ^{18}O may not faithfully register total rainfall at a particular site [*Baker et al.*, 2007]. Focusing on the broad changes in atmospheric circulation and correlations with ice core records, *Wang et al.* [2001] proposed that Hulu speleothem δ^{18}O could represent "monsoon intensity"; that is, regional changes of moisture sources and rainfall patterns, which was confirmed by subsequent studies on many other Chinese cave sites [*Hu et al.*,

[1]Key Laboratory of Cenozoic Geology Environment, Institute of Geology and Geophysics, Chinese Academy of Sciences, Beijing, China.
[2]Now at National Research Center for Geoanalysis, Beijing, China.
[3]Faculty of Environment and Resource Studies, Mahidol University, Nakhom Pathom, Thailand.
[4]College of Geography Science, Nanjing Normal University, Nanjing, China.
[5]Institute of Climate System, Chinese Academy of Meteorological Sciences, Beijing, China.

0148-0227/10/2009JD013378

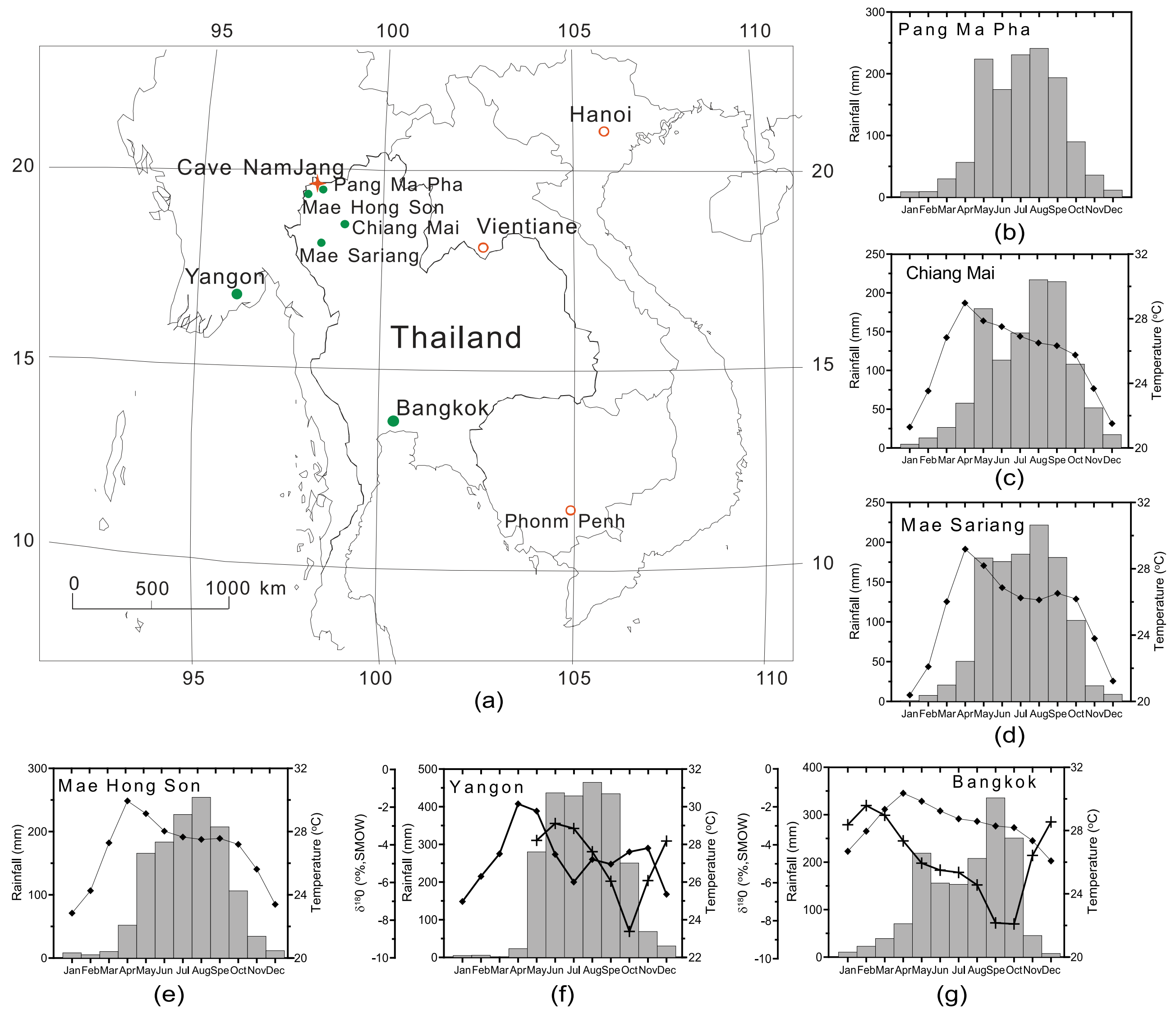

Figure 1. (a) Map of the study region showing Namjang cave and the meteorological observation stations in the region. (b) Mean monthly rainfall at Pang Ma Pha (19°31′N, 98°15′E). (c) Mean monthly rainfall and temperature (solid line with diamond points) at Chiang Mai (18°47′N, 98°59′E). (d) Mae Sariang (18°10′N, 97°56′E) and (e) Mae Hong Son (19°18′N, 97°50′E). Mean monthly rainfall (gray bar), δ^{18}O value (solid line with crosses), and temperature (solid line with diamonds) at (f) Yangon (16°46′N, 96°10′E) and (g) Bangkok (13°44′N, 100°34′E).

2008; *Wang et al.*, 2001, 2005, 2008; *Yuan et al.*, 2004; *Zhang et al.*, 2008].

[3] Another approach to examine the climate signature imprinted in stalagmites is to compare the most recent δ^{18}O variations to the modern instrumental data [*Baker et al.*, 2007] and investigate to what degree speleothem δ^{18}O can represent monsoonal rainfall. To this end, an active, annually laminated stalagmite from northwestern Thailand, covering recent 105 years, was analyzed. Thailand and its neighboring Indochinese Peninsula are located at a transition zone between two tropical monsoon subsystems (Indian and western North Pacific) [*Wang and Ho*, 2002]. Records with equivalent qualities are still scarce in Southeast Asia. The distinct annual laminae preserved in this stalagmite allow us to establish an annual lamina-based multiproxy record, and then compare it with local instrumental data to examine the detailed correlation between speleothem δ^{18}O and monsoonal rainfall.

2. Site Descriptions

[4] Namjang cave (98°12′12″E, 19°40′30″N, elevation ~923 m at the entrance) is located in Pang Ma Pha, Mae Hong Son Province, Thailand (Figure 1a). It was developed in Permian limestone and dolostone formation. The vegetation above the cave is made up of mixed deciduous forest. The cave is ~65 m long and ~6 m wide, with an entrance of ~4 m high and ~1 m wide. The relative humidity is ~80% inside the cave during the early rainy season of 2009. Stalagmite NJ-1 was collected ~18 m away from the cave entrance and ~9 m above the floor in April 2006.

[5] The mean annual precipitation is of ~1300 mm, and mean annual temperature is 27°C. In this area, monsoonal rainfall season initiates in May and continues through October, followed by a dry season from November to April. The total rainfall during the monsoon season contributes more than 90% of the mean annual rainfall. However, rainfall amount is characterized by heterogeneous intra-seasonal patterns in the region. For example, the rainfall data from the closest meteorological station Pang Ma Pha (1987–2006 A.D.) (Figure 1b), which is ~19 km southeast from the cave, show a bipeak distribution, with a primary peak in August and the secondary maximum in May. This bipeak feature is also registered in other stations, such as Chiang Mai (Figure 1c) and Bangkok (Figure 1g), located toward the southeast of the study site. On the contrary, another meteorological station Mae Hong Son (rainfall data from 1911 to 2002 A.D.; see Figure 1e), which is ~45 km southwest from the cave, shows a monopeak distribution, with a peak of ~250 mm in August. This monsoonal rainfall distribution is similar with that from Yangon, Burma (Figure 1f), and the observations at Mae Sariang, Mae Hong Son, located at the eastern slope of mountain between Burma and Thailand (Figure 1d).

[6] Nevertheless, these two groups of sites show nearly identical seasonal rainfall $\delta^{18}O$. For instance, in Bangkok, rainfall $\delta^{18}O$ shifts from ~−5.3 ‰ in early monsoon season to less than −8‰ during the later monsoon season. In Yangon, it shows similar much negative values of $\delta^{18}O$ in the later season, even though the seasonal rainfall pattern is different with that of Bangkok. These indicate that rather than the so-called "amount effect," other factors, such as moisture source or monsoon circulation could control rainfall $\delta^{18}O$ at the study site. The different monsoonal rainfall distributions, yet similar rainfall $\delta^{18}O$ between the two neighboring meteorological stations, strongly suggests that the regional climate is under the influence of the same monsoon system, and the local precipitation isotopic signature can represent variations of monsoon intensity in much broader region. Since the rainfall isotopic data in Mae Hong Son and Pang Ma Pha are not available, we plotted here the average monthly climate data from Bangkok (1968–2004 A.D.) and Yangon (1961–1963 A.D.; see IAEA/WMO's Global Network of Isotopes in Precipitation: The GNIP Database at http://www.iaea.org/water), including isotope composition, and applied them as references for the isotopic component of regional precipitation (Figures 1f and 1g).

3. Methods

[7] The columnar stalagmite NJ-1, 41 cm in height and ~6 cm in diameter, was halved and one of the cut sections was polished. In this study, only the topmost 26 mm was analyzed. XRD analysis revealed that crystals in the stalagmite were aragonite. The sample has clear visible laminae in hand section (Figure 2). Each lamina is composed of white porous aragonite and subtransparent dense aragonite couplet. In the couplets, the dense portion has a relatively constant thickness, while thickness of porous part can have significant changes (Figure 2d).

[8] The polished section of stalagmite was scanned using a precalibrated high-resolution scanner at RGB/3200 dpi conditions. The digital image was then applied for lamina analysis. Visible laminae were marked and counted using Adobe Photoshop software. Laminae thickness were measured using Image-Pro Plus 5.1 software, and calculated by measuring the average distance between visible laminae using a ~0.4 mm wide transect, followed the protocols previously described in the work of *Baker et al.* [2007].

[9] A total of 234 subsamples were prepared for stable isotope analysis. Twenty-five subsamples were drilled along growth horizons for the "Hendy Test" [*Hendy*, 1971] using a 0.5 mm carbide dental burrs. The rest of 209 subsamples were milled along the growth axis continuously at an interval of ~125 microns, using a stainless steel surgical blade. After each sampling, the blade and milling surface were cleaned with a stream of compressed air, and the blade was further cleaned with anhydrous ethanol. In order to mark the location of each subsample, the milling surface was routinely scanned. Stable isotope analyses were performed on a MAT-253 mass spectrometer (Thermo-Finnigan) linked to a Kiel III automated carbonate reaction device at Nanjing Normal University, China. The values are reported in parts per thousand (‰) with respect to the Vienna Pee Dee Belemnite (VPDB) standard. Analytical precision was better than 0.1‰.

[10] In order to confirm the continual deposition of the study section of NJ-1 and annual feature of the laminae, two powder samples were drilled for ^{230}Th dating at 4.0 and 24.5 mm from the top, respectively. These two samples, weighed ~100 mg, were drilled along growth bands using a 0.9 mm diameter carbide dental burr. Chemical separation procedures and isotopic measurements were made at the Department of Geology and Geophysics, University of Minnesota, following *Shen et al.* [2002].

4. Results and Discussions

4.1. Stalagmite Lamina Chronology

[11] NJ-1 was collected at the end of dry season in April 2006. The U-Th dating effort at its top was unfortunately not successful, probably owing to its very young age, but high content of detrital material (Figure 2a). However, the sample was receiving active dripping. The topmost lamina can therefore be reasonably set to 2005 A.D., presumably forming during the rainy season of 2005 to the dry season of 2006. A total of 105 laminae were counted in the topmost 26 mm of NJ-1. The sampling interval for the ^{230}Th age is centered at 24.5 mm (24.0–25.0 mm) and covers the 98–104th laminae, equivalent to a time period of 1902–1908 A.D. This agrees well with the ^{230}Th dating result of 1893 ± 21 A.D. (Table 1), indicating that laminae in NJ1 are annual and the deposition is most likely continual from the dating point to the top. Therefore, we can apply lamina counting to establish the calendar chronology for the $\delta^{18}O$ profile in annual resolution. We then assigned each $\delta^{18}O$ data point an age through comparing scanned images of $\delta^{18}O$ subsample position with the whole image of the studied section on which the lamina was labeled. Sampling approach for stable isotope analysis in this study yields 1–5 $\delta^{18}O$ data per year, varying with the laminar thickness. In the case that several $\delta^{18}O$ data were derived from one lamina, the averaged values were applied to establish an annual data set for comparing with instrument data (Figure 3).

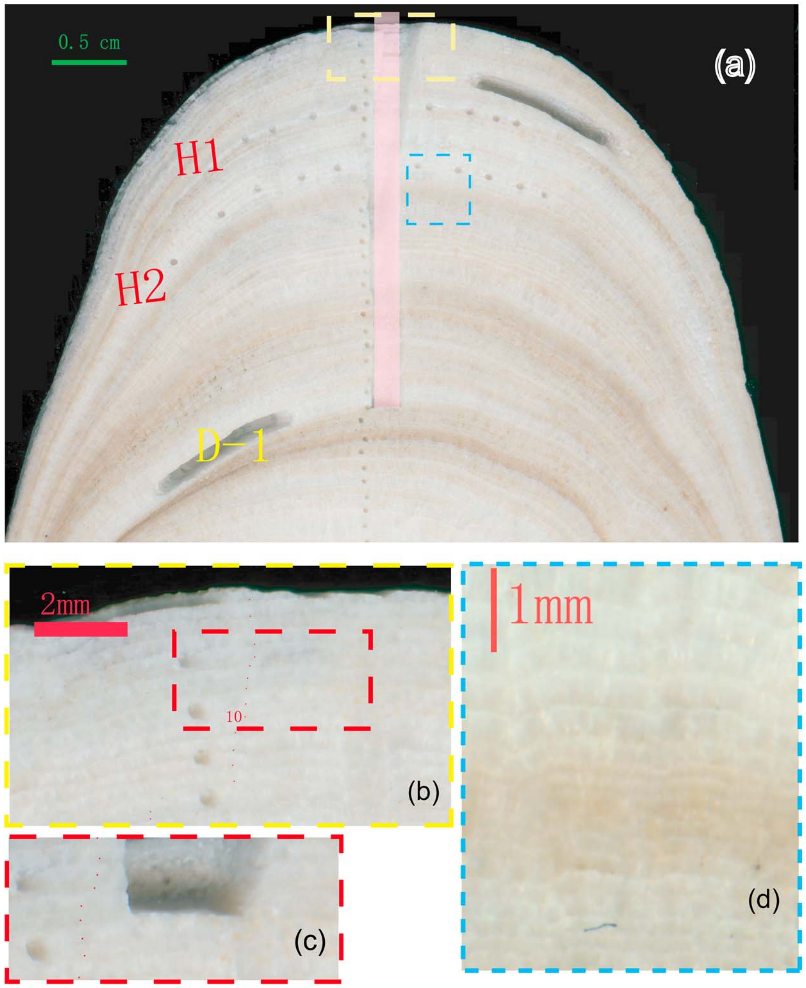

Figure 2. (a) Polished sections of stalagmite NJ-1. Samples for Hendy tests were drilled along laminae (labeled "H-1" and "H-2"), the sample for ^{230}Th dating was horizontal drilled along laminae (labeled "D-1"), and samples for oxygen isotope profile were vertically milled along growing axis (marked by pink bar). (b–c) Amplified images show the annual laminae which have been labeled (Figure 2b) and routinely scanned image after a subsample for isotopes analysis was milled (Figure 2c). (d) Amplified image shows the variance of laminae thickness.

4.2. Variation in δ^{18}O and Growth Rate

[12] In the top section of NJ-1, δ^{18}O varies between −6.8‰ and −3.3‰, and growth rate varies from 0.10 mm/y to 0.53 mm/y (Figure 3e). They exhibit similar decadal variability, with more negative δ^{18}O values coinciding with thicker laminae. The strong relationships are also shown in the Pearson correlation analysis test ($r = -0.72$, $P < 0.001$). In the δ^{18}O profile, three distinct intervals can be identified, with relatively negative values, corresponding to peaks in growth rate. They occurred at approximately 1903–1907 A.D., 1946–1956 A.D. and 1973–1985 A.D., with values drop by ~2–2.5‰.

4.3. Comparisons With Instrumental Data

[13] To examine the climate signal in δ^{18}O and growth rate series of stalagmite NJ-1, we first compared them with annual, seasonal, and monthly instrumental rainfall data. We only listed here the monthly data for April through November, because rainfall is virtually negligible in other months (Table 2). Considering that drip water may lag in

Table 1. ^{230}Th Dating Result From Stalagmite NJ-1 From Namjang Cave, Thailand[a]

Depth (mm)	^{238}U (ppb)	^{232}Th (ppt)	^{230}Th/^{232}Th (ppm)	Measured δ^{234}U	Activity ^{230}Th/^{238}U	Uncorrected ^{230}Th age (y)	Corrected ^{230}Th Age (YBP)	Corrected ^{230}Th Age (A.D.)	Corrected $\delta^{234}U_{Initial}$
24.5	1018 ± 2	3737 ± 16	17 ± 1	1743 ± 4	0.00383 ± 0.00018	152 ± 7	57 ± 21	1893 ± 21	1744 ± 4

[a]Errors are 2σ errors. Decay constant values are: $\lambda_{230} = 9.1577 \times 10^{-6}$ y^{-1}, $\lambda_{234} = 2.8263 \times 10^{-6}$ y^{-1} [*Cheng et al.*, 2000], and $\lambda_{238} = 1.55125 \times 10^{-10}$ y^{-1} [*Jaffey et al.*, 1971]. Corrected ^{230}Th ages assume the initial ^{230}Th/^{232}Th atomic ratio of $4.4 \pm 2.2 \times 10^{-6}$. Depths along the growth axis are relative to the top of the stalagmite. YBP, year before present (1950 A.D.).

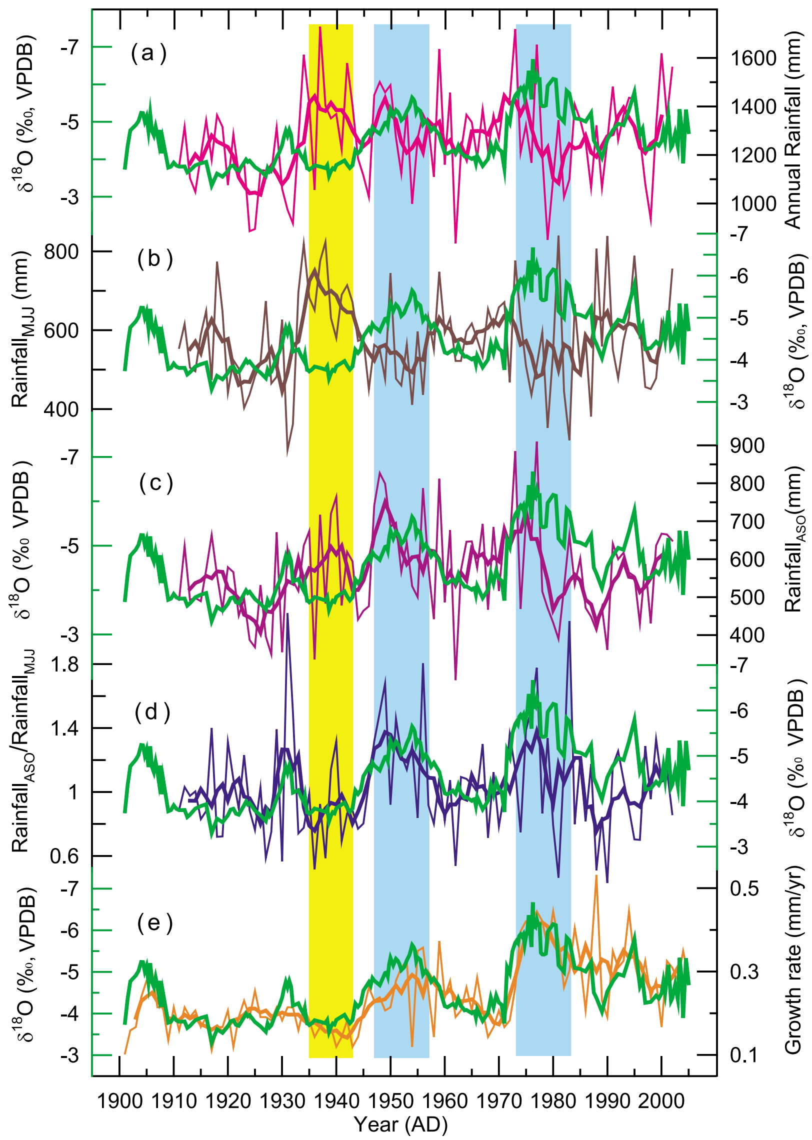

Figure 3. Comparisons of NJ-1 δ^{18}O record (dark green curve) with Mae Hong Son instrumental record (Figures 3a–3d) and lamina thickness (orange curve in Figure 3e). (a) Annual rainfall (magenta). (b) Total rainfall in May–July (MJJ) (dark brown). (c) Total rainfall in August–October (ASO) (purple). (d) Ratio of later monsoon rainfall (ASO) to early monsoon rainfall (MJJ) (blue). Bold lines indicate 5 year moving average trends. The yellow bar shows the interval of more annual rainfall but lower proportional ASO rainfall, corresponding to the positive valley in NJ-1 δ^{18}O record. Cyan bars show two negative peaks in NJ-1 δ^{18}O record, which correspond to higher proportional ASO rainfall.

terms of responding surface rainfall, we also compared the stalagmite δ^{18}O with prior year rainfall data (Table 2). As our sampling approach may have partially mixed materials from nearby laminae where growth rate is relatively low, and also because the existence of groundwater could smooth out seasonal rainfall signal when the fluid passes through the vadose zone [*Baker et al.*, 2007; *Fairchild et al.*, 2006], we plotted the annual-scale δ^{18}O and growth rate profiles against with 5 year moving averages of the rainfall data (see Figure 3 and Table 2). For comparison purposes, we further divided the monsoonal rainfall season into early rainfall season from May to July (MJJ) and later season, covering August to October (ASO).

[14] One observation clearly standing out is that the correlations vary between speleothem δ^{18}O and different monthly rainfall time series. For example, a negative correlation can be found between the time series of δ^{18}O and September rainfall at Mae Hong Song ($r = -0.25$, $p < 0.05$), whereas weak positive relationship exists between the δ^{18}O and the July rainfall. Although we could not rule out the possibility that the drip water may lag local rainfall, this time lag is likely to be small owing to the existence of the annual banding in the sample. Further, when we shifted the sample δ^{18}O data 1 year ahead and compared with the instrumental rainfall data, we only found a slightly better correlation (Table 2). Nevertheless, we propose here to use a 5 year smoothed climate data for the comparison. This

Table 2. Pearson Correlations (r Values) Between Mae Hong Son Rainfall Data and Stalagmite $\delta^{18}O$ and Growth Rate Values

Month and Season	Prior Year Rainfall		Current Year Rainfall		5 Year Averaged Rainfall	
	Growth Rate	$\delta^{18}O$	Growth Rate	$\delta^{18}O$	Growth Rate	$\delta^{18}O$
April	0.00	−0.10	0.07	−0.05	0.02	−0.12
May	−0.10	0.05	−0.06	0.09	−0.11	0.19
June	−0.07	0.04	0.02	0.05	−0.14	0.05
July	**−0.22**	**0.29**	−0.04	0.15	**−0.26**	**0.36**
August	−0.08	−0.05	0.03	−0.05	−0.14	−0.01
September	0.07	**−0.29**	**0.20**	**−0.25**	0.08	**−0.43**
October	0.02	−0.03	−0.03	−0.05	0.13	−0.15
November	0.07	0.01	0.07	−0.01	0.01	0.04
Annual	−0.06	−0.08	0.11	−0.09	−0.08	−0.12
May–October (M-O)	−0.14	−0.02	−0.14	−0.04	0.06	−0.04
May–July (MJJ)	**−0.21**	**0.21**	−0.04	0.16	**−0.26**	**0.30**
August–October (ASO)	0.01	**−0.22**	0.13	**−0.20**	0.03	**−0.33**
ASO/Annual	0.07	**−0.23**	0.07	**−0.20**	0.11	**−0.39**
ASO/MJJ	0.17	**−0.31**	0.15	**−0.30**	**0.22**	**−0.50**
ASO/M-O	0.15	**−0.30**	0.13	**−0.26**	0.19	**−0.48**

Statistically significant values ($p < 0.05$) are shown in bold.

would be a reasonable compromise when we further incorporate both the dating error and the uncertainty on band accounting, which is confirmed by the significantly increased correlation between the two data sets (Table 2). Because monsoonal rainfall has intraseasonal variation, we applied a ratio of ASO to MJJ rainfall, and observed a stronger relationship with the speleothem $\delta^{18}O$ on an annual basis ($r = -0.30$, $p < 0.01$) (Table 2). When compared with 5 years smoothed rainfall data, this correlation is even higher ($r = -0.50$, $p < 0.001$) (Table 2). In particular, from 1934 A.D. to 1943 A.D., the relatively high NJ-1 $\delta^{18}O$ (~−3.8‰) correlated remarkably with elevated annual rainfall of ~1400 mm and MJJ rainfall of ~680 mm, but normal ASO rainfall of ~610 mm (Figure 3). On the contrary, negative peak in NJ-1 $\delta^{18}O$ (~−5.4‰) during the period of 1946–1956 A.D. is corresponded to low annual and MJJ rainfalls (~1230 and ~510 mm, respectively), but higher ASO rainfall of ~700 mm (Figure 3).

[15] The growth rate in NJ-1 shows somewhat significantly positive correlation with September rainfall ($r = 0.20$, $p < 0.05$) (see Table 2 and Figure 3). Contrary to $\delta^{18}O$, the growth rate is positively correlated with the 5 year smoothed ASO/MJJ rainfall ratio ($r = 0.22$, $p < 0.05$) (Table 2). The correlation practice suggests that the variability of sample growth rate is probably determined by the rainfall in the later monsoon season from August through October.

4.4. Understanding the Variation in $\delta^{18}O$ and Growth Rate

[16] The "Hendy Test" results [*Hendy*, 1971] (Figure 4) show that the $\delta^{18}O$ value has little variation along single lamina, although $\delta^{13}C$ and $\delta^{18}O$ are positively correlated along the growth axis. The negative correlation between the growth rate and the $\delta^{18}O$ also suggests that the possible disequilibrium fractionation during fast degassing and aragonite precipitation did not override the climate signal of NJ-1 $\delta^{18}O$ series, which was also found in stalagmite from the Austrian Alps [*Spötl and Mangini*, 2002]. With the current cave temperature and annual mean precipitation $\delta^{18}O$, we can calculate the potential aragonite $\delta^{18}O$ assuming the mineral is precipitated under equilibrium conditions [*Kim et al.*, 2007]. The estimated value is somewhat about 4‰ lower than the averaged aragonite $\delta^{18}O$ in our sample, which suggested a significant contribution of kinetic effects to our sample isotopic signal. Nevertheless, as we argued above and confirmed by the climate correlation discussed below, the $\delta^{18}O$ value of stalagmite NJ-1 is likely dominated by the averaged $\delta^{18}O$ of recharging rainfall and some effects of the cave air temperature. Since the temperature-dependent change in speleothem $\delta^{18}O$ is likely minor owing to the shallow slope of the aragonite/water fractionation-temperature curve (−0.20 ‰/°C; see *Kim et al.* [2007]), the large amplitude of $\delta^{18}O$ shift (up to 4 ‰) should primarily record the isotopic composition change in rainfall.

[17] Rainfall in the region is under the influence of the Asian Monsoon system and is associated with the movement of the Intertropical Convergence Zone (ITCZ). The monsoon onsets in May and brings warm and moist airstreams from the Indian Ocean toward Thailand. The ITCZ is located above southern Thailand in May, resulting in a rainfall peak in the region. In August, the ITCZ penetrates further north and lies over northern and northeastern Thailand, and then gradually shifts southward to central Thailand in September and southern parts in October, which leads to the major rainfall peak during August to October [*Singhrattna et al.*, 2005], and contributes more than 45% of annual precipitation in the region.

[18] This later monsoon rainfall is characterized with lighter $\delta^{18}O$ (average ~−7.5‰ at Bangkok, and ~−6.3‰ at Yangon). On the contrary, the early monsoon rainfall from May to July, although it also delivers nearly 45% of the annual precipitation in the region, registers relatively heavy $\delta^{18}O$, with average ~−5.3‰ at Bangkok and ~−3.3‰ at Yangon. The regional rainfall in dry season from November to next April is in general less than 10% of the annual rainfall, so their contribution to groundwater is probably negligible. This intraseasonal variation in rainfall $\delta^{18}O$ can be captured in cave drip water, therefore, faithfully recorded in cave deposits, as observed in the strong negative correlation between NJ-1 $\delta^{18}O$ and the ASO/MJJ rainfall ratio (see Table 2 and Figure 3d).

[19] Higher ASO rainfall can maintain drip water at higher level in following dry season, in turn increase the growth

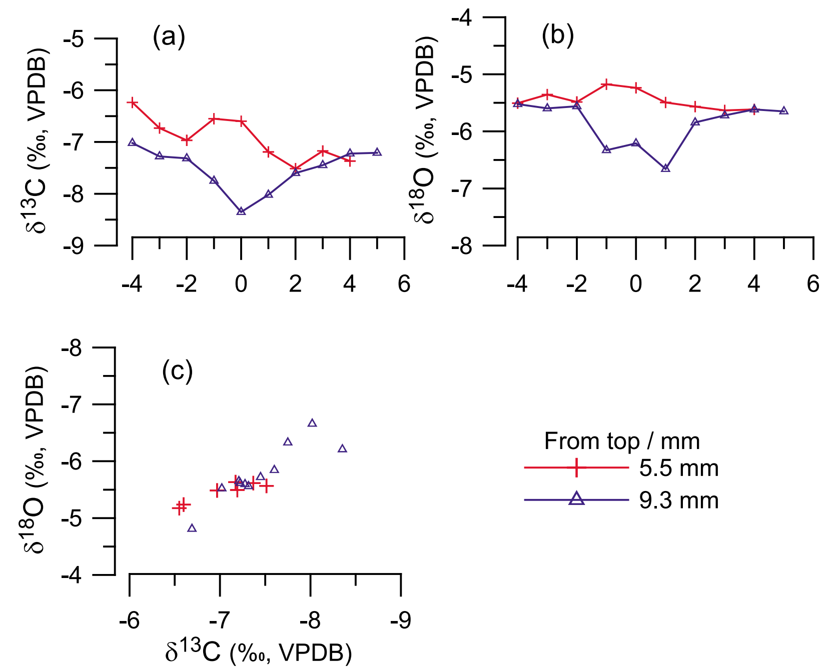

Figure 4. Hendy test of stalagmite (a) NJ-1 δ^{13}C and (b) δ^{18}O along the same layer plotted against distance from the growth axis. Units for the *x* axes are sample number, with "zero" indicating the sample on the growth axis, and the approximate distance from one end of each five sample set to the other is about 1 cm along a growth horizon. (c) Relationship of δ^{13}C and δ^{18}O along both the profile (magenta square) and the same layer.

rate of stalagmite, because drip rate is a key factor for stalagmite growth when the drip rate is low [*Genty et al.*, 2001], less dripping would lead to a reduced growth rate in cave deposits [*Baker et al.*, 2007]. This is consistent with our observation that a positive correlation exists between the Thailand late monsoonal rainfall and NJ-1 growth rate.

[20] The difference on δ^{18}O value of seasonal monsoon rainfall probably originates from the distinctive moisture sources and associated large-scale monsoon circulations, which can be closely resembled by the background climatic mean water vapor transport in the lower troposphere. On the basis of the NCEP/NCAR Reanalysis data [*Kalnay et al.*, 1996], vertically integrated climate mean (1948–2005 average) MJJ and September–October (SO) water vapor transports were estimated (Figure 5). Generally, the water vapor supply related to MJJ rainfall is different from that related to SO rainfall. Moisture from the Indian Ocean, especially from the Bay of Bengal, dominantly support the MJJ rainfall in this region (Figure 5a), while SO rainfall is favored by convergence of the moisture coming from the South China Sea, ultimately originated from the WPWP, with somewhat water vapor contribution from the Indian Ocean (Figure 5b). It seems that rainfall associated with the western North Pacific summer monsoon circulation [*Wang and Ho*, 2002] in this region has relatively negative δ^{18}O values than that originated from the Indian Ocean. The detail mechanism for this difference is still unknown, and its fully understanding would require more observation data and modeling efforts on moisture source and its effect on meteoric water δ^{18}O in the region.

[21] Paleoclimate records produced from speleothems can be superior to other proxy records because of their precise

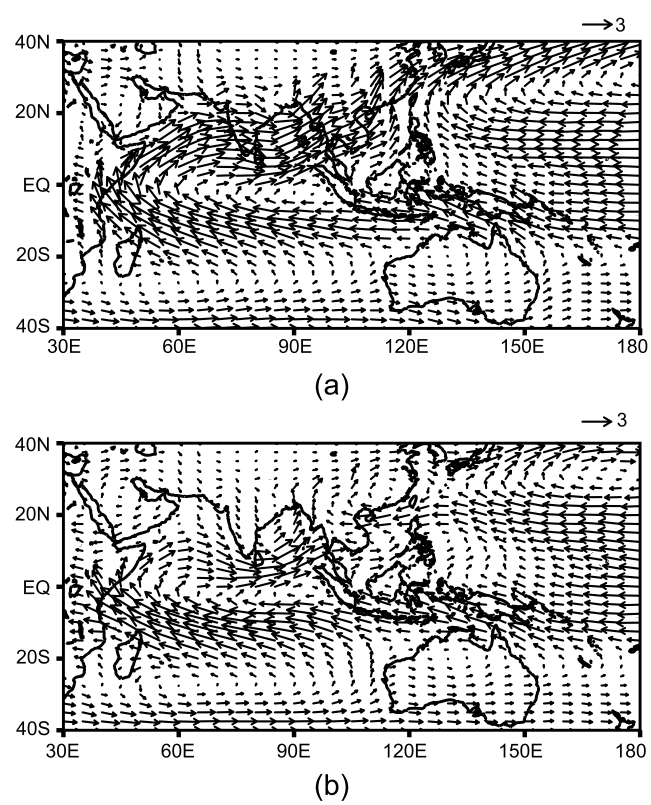

Figure 5. Vertically integrated climate mean (1948–2005 average) (a) May–July and (b) September and October water vapor transport (10^5 g cm^{-1} s^{-1}) based on NCEP-NCAR reanalysis.

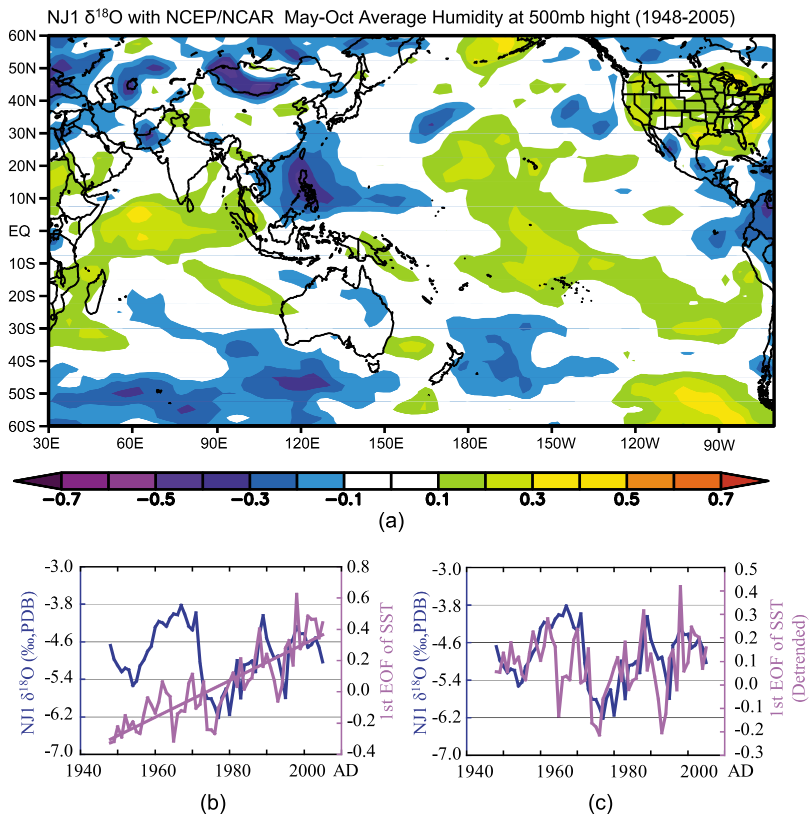

Figure 6. (a) Correlation of NJ1 δ^{18}O with NCEP/NCAR reanalysis average May–October 500 mb relative humidity (1948–2005). Image provided by the NOAA/ESRL Physical Sciences Division (PSD), Boulder, Colorado (http://www.esrl.noaa.gov/psd/). (b) Comparison between the NJ1 δ^{18}O and the Pacific Warm Pool Index (first EOF of SST over 60–170°E, 15°S–15°N; data were downloaded from NOAA/ESRL PSD, and yearly mean values were used). (c) Same as Figure 6b except for detrended first EOF of SST.

chronological control. The interpretation of its proxy, such as δ^{18}O, however is not always without ambiguity [*Lachniet*, 2009]. In the tropics, speleothem δ^{18}O is typically suggested to indicate local rainfall amount [*Burns et al.*, 2001, 2002]. There is a recent tendency to apply speleothem δ^{18}O as a proxy of monsoon intensity [*Wang et al.*, 2001, 2005, 2008] or ITCZ migration [*Fleitmann et al.*, 2007]; that is, change of regional atmospheric circulation. Similarly, our NJ-1 record shows a rather poor correlation with the total rainfall amount. Instead, the speleothem δ^{18}O is well correlated with the ASO/MJJ rainfall ratio. As moisture sources or monsoon circulations that give rise to ASO rainfall and MJJ rainfall maybe different, the variation of NJ-1 δ^{18}O could indicates the relative intensity of different monsoon subsystems; that is, Indian and western North Pacific summer monsoon [*Wang and Ho*, 2002]. Because ASO rainfall is the primary peak in this region, and it sustains the continually growth of lamina through the following dry season, which is further confirmed by the positive correlation between our sample growth rate and September rainfall, the ASO rainfall has the primary control in the climate signal of NJ-1 δ^{18}O. The lighter speleothem δ^{18}O implies more proportion of ASO rainfall; that is, a stronger Thailand Monsoon (defined as ASO rainfall; see *Singhrattna et al.* [2005]).

4.5. Correlation With Large-Scale Circulation Variability

[22] In order to investigate the cause of the decadal variation of NJ-1 δ^{18}O, we compared our stalagmite data with the average May to October humidity at 500 mb height over the Pacific and the Indian Oceans (Figure 6a). The negative correlation with the WPWP humidity is clear, with higher humidity at 500 mb height over the Philippines and the South China Sea correlating to more negative values of NJ-1 δ^{18}O. The positive correlation was shown from the central Indian Ocean. This result is consistent with our proposed mechanisms that the NJ-1 δ^{18}O is controlled by moisture from both the Indian Monsoon and the western North Pacific summer monsoon, and the latter has a dominant effect. The major contribution of the western North Pacific summer monsoon in our speleothem record was further supported by the closely relationship between the NJ-1 δ^{18}O record and the WPWP index, the first EOF of SST calculated by Matin P. Hoerling (personal communication, 2010), especially for the time period after the mid-1970s (Figures 6b and 6c). Associated with the well-known shift of PDO in 1976–1977 [*Graham*, 1994], it seem that the PDO perhaps played a role in this decadal variance. Interestingly, an inverse statistic relationship between NJ-1 δ^{18}O and PDO was shown for time period prior to 1976 and post-

1976, with positive correlation for pre-1976 (1911–1976, $r = -0.51$, $p < 0.001$) and negative correlation for post-1976 (1977–2005, $r = 0.35$, $p < 0.05$). However, the physical mechanism for these complex connections with the WPWP, the Indian Ocean and PDO are still unknown. Further studies, including applying ocean-atmosphere coupled models, will be needed to understand this decadal variance.

5. Conclusions

[23] A 105-year long, annual laminated stalagmite record from Namjang cave, northwestern Thailand, allows us for the first time to examine the relationship between its $\delta^{18}O$ values with instrumental data in details. The speleothem $\delta^{18}O$ record surprisingly has a rather poor correlation with annual rainfall amount. Instead, its lower values were found to coincided with the relative rainfall amount in the later monsoon season, indexed here as the ratio of ASO/MJJ rainfalls, and may reflect the relative intensity of the western North Pacific summer monsoon and the Indian Monsoon. The stalagmite growth rate primarily reflects local rainfall in later rainy season, corresponding negatively with the speleothem $\delta^{18}O$ value. Our sample $\delta^{18}O$ therefore can be used as a proxy of ASO rainfall at a time when the monsoonal rainfall reaches peaks in the Indochinese Peninsulas. The results challenge a simple practice that uses speleothem $\delta^{18}O$ as an indicator of rainfall amount, but suggest that intraseasonal variation of summer monsoon rainfall plays an important role on stalagmite $\delta^{18}O$, particularly for cave records from the transition zone of submonsoon systems. The decadal variance of our speleothem $\delta^{18}O$ record is likely related to the oceanic-atmospheric processes over the WPWP, and possibly modulated by decadal variability of large-scale circulation; for example, PDO. Further studies including applying ocean-atmosphere coupled model, will be need to completely characterize these effects.

[24] **Acknowledgments.** We thank R. L. Edwards and Hai Cheng for their support on the ^{230}Th dating. We are grateful for the friendly help of local people. B. Cai is in debt to Luo Wang and Qiangzhen Hao for their constructive comments and valuable discussions. This research is supported by National Basic Research Program of China grant 2010CB950201 and 2010CB950101, China NSFC grants 40772213 and 40602021, and National Research Council Thailand (2008–2010). We especially thank anonymous reviewers for their constructive suggestions that improved this contribution considerably.

References

Baker, A., A. Asrat, I. J. Fairchild, M. J. Leng, P. M. Wynn, C. Bryant, D. Genty, and M. Umer (2007), Analysis of the climate signal contained within delta O-18 and growth rate parameters in two Ethiopian stalagmites, *Geochim. Cosmochim. Acta*, *71*, 2975–2988, doi:10.1016/j.gca.2007.03.029.

Burns, S. J., D. Fleitmann, A. Matter, U. Neff, and A. Mangini (2001), Speleothem evidence from Oman for continental pluvial events during interglacial periods, *Geology*, *29*, 623–626, doi:10.1130/0091-7613(2001)029<0623:SEFOFC>2.0.CO;2.

Burns, S. J., D. Fleitmann, M. Mudelsee, U. Neff, A. Matter, and A. Mangini (2002), A 780-year annually resolved record of Indian Ocean monsoon precipitation from a speleothem from south Oman, *J. Geophys. Res.*, *107*(D20), 4434, doi:10.1029/2001JD001281.

Cai, B. G., R. L. Edwards, H. Cheng, M. Tan, X. Wang, and T. S. Liu (2008), A dry episode during the Younger Dryas and centennial-scale weak monsoon events during the early Holocene: A high-resolution stalagmite record from southeast of the Loess Plateau, China, *Geophys. Res. Lett.*, *35*(2), L02705, doi:10.1029/2007GL030986.

Cheng, H., R. L. Edwards, J. Hoff, C. D. Gallup, D. A. Richards, and Y. Asmerom (2000), The half-lives of uranium-234 and thorium-230, *Chem. Geol.*, *169*, 17–33, doi:10.1016/S0009-2541(99)00157-6.

Fairchild, I. J., C. L. Smith, A. Baker, L. Fuller, C. Spotl, D. Mattey, F. McDermott, and E. I. M. F. (2006), Modification and preservation of environmental signals in speleothems, *Earth Sci. Rev.*, *75*, 105–153, doi:10.1016/j.earscirev.2005.08.003.

Fleitmann, D., et al. (2007), Holocene ITCZ and Indian monsoon dynamics recorded in stalagmites from Oman and Yemen (Socotra), *Quat. Sci. Rev.*, *26*, 170–188, doi:10.1016/j.quascirev.2006.04.012.

Genty, D., A. Baker, and B. Vokal (2001), Intra- and inter-annual growth rate of modern stalagmites, *Chem. Geol.*, *176*, 191–212, doi:10.1016/S0009-2541(00)00399-5.

Graham, N. E. (1994), Decadal-scale climate variability in the tropical and North Pacific during the 1970s and 1980s: Observations and model results, *Clim. Dyn.*, *10*, 135–162, doi:10.1007/BF00210626.

Hendy, C. H. (1971), The isotopic geochemistry of speleothems—I. The calculation of the effects of different modes of formation on the isotopic composition of speleothems and their applicability as palaeoclimatic indicators, *Geochim. Cosmochim. Acta*, *35*, 801–824, doi:10.1016/0016-7037(71)90127-X.

Hu, C., G. M. Henderson, J. Huang, S. Xie, Y. Sun, and K. R. Johnson (2008), Quantification of Holocene Asian monsoon rainfall from spatially separated cave records, *Earth Planet. Sci. Lett.*, *266*, 221–232, doi:10.1016/j.epsl.2007.10.015.

Intergovernmental Panel on Climate Change (IPCC) (2007), Summary for policymakers, in *Climate Change 2007: Impacts, Adaptation and Vulnerability. Contribution of Working Group II to the Fourth Assessment Report of the Intergovernmental Panel on Climate Change*, edited by M. L. Parry et al., pp. 7–22, Cambridge Univ. Press, New York.

Jaffey, A. H. K., F. Flynn, L. E. Glendenin, W. C. Bentley, and A. M. Essling (1971), Precision measurement of half-lives and specific activities of $^{235}U$and ^{238}U, *Phys. Rev. C*, *4*, 1889–1906, doi:10.1103/PhysRevC.4.1889.

Kalnay, E., et al. (1996), The NCEP/NCAR Reanalysis 40-year project, *Bull. Am. Meteorol. Soc.*, *77*, 437–471, doi:10.1175/1520-0477(1996)077<0437:TNYRP>2.0.CO;2.

Kim, S. T., J. R. O'Neil, C. Hillaire-Marcel, and A. Mucci (2007), Oxygen isotope fractionation between synthetic aragonite and water: Influence of temperature and Mg2+ concentration, *Geochim. Cosmochim. Acta*, *71*, 4704–4715, doi:10.1016/j.gca.2007.04.019.

Lachniet, M. S. (2009), Climatic and environmental controls on speleothem oxygen-isotope values, *Quat. Sci. Rev.*, *28*, 412–432, doi:10.1016/j.quascirev.2008.10.021.

McDermott, F. (2004), Palaeo-climate reconstruction from stable isotope variations in speleothems: A review, *Quat. Sci. Rev.*, *23*, 901–918, doi:10.1016/j.quascirev.2003.06.021.

Shen, C.-C., R. L. Edwards, H. Cheng, J. A. Dorale, R. B. Thomas, S. Bradley Moran, S. E. Weinstein, and H. N. Edmonds (2002), Uranium and thorium isotopic and concentration measurements by magnetic sector inductively coupled plasma mass spectrometry, *Chem. Geol.*, *185*, 165–178, doi:10.1016/S0009-2541(01)00404-1.

Singhrattna, N., B. Rajagopalan, K. K. Kumar, and M. Clark (2005), Interannual and interdecadal variability of Thailand summer monsoon season, *J. Clim.*, *18*, 1697–1708, doi:10.1175/JCLI3364.1.

Spötl, C., and A. Mangini (2002), Stalagmite from the Austrian Alps reveals Dansgaard-Oeschger events during isotope stage 3: Implications for the absolute chronology of Greenland ice cores, *Earth Planet. Sci. Lett.*, *203*, 507–518, doi:10.1016/S0012-821X(02)00837-3.

Tan, M., T. Liu, J. Hou, X. Qin, H. Zhang, and T. Li (2003), Cyclic rapid warming on centennial-scale revealed by a 2650-year stalagmite record of warm season temperature, *Geophys. Res. Lett.*, *30*(12), 1617, doi:10.1029/2003GL017352.

Wang, B., and L. Ho (2002), Rainy season of the Asian-Pacific summer monsoon, *J. Clim.*, *15*, 386–398, doi:10.1175/1520-0442(2002)015<0386:RSOTAP>2.0.CO;2.

Wang, Y., H. Cheng, R. L. Edwards, Z. An, J. Wu, C. C. Shen, and J. A. Dorale (2001), A high-resolution absolute-dated late Pleistocene monsoon record from Hulu cave, China, *Science*, *294*, 2345–2348, doi:10.1126/science.1064618.

Wang, Y., H. Cheng, R. L. Edwards, Y. He, X. Kong, Z. An, J. Wu, M. J. Kelly, C. A. Dykoski, and X. Li (2005), The Holocene Asian monsoon: Links to solar changes and North Atlantic climate, *Science*, *308*, 854–857, doi:10.1126/science.1106296.

Wang, Y., H. Cheng, R. L. Edwards, X. Kong, X. Shao, S. Chen, J. Wu, X. Jiang, X. Wang, and Z. An (2008), Millennial- and orbital-scale changes in the east Asian monsoon over the past 224,000 years, *Nature*, *451*, 1090–1093, doi:10.1038/nature06692.

Yuan, D., et al. (2004), Timing, duration, and transitions of the last interglacial Asian monsoon, *Science*, *304*, 575–578, doi:10.1126/science.1091220.

Zhang, P. Z., et al. (2008), A test of climate, sun, and culture relationships from an 1810-year Chinese cave record, *Science*, *322*, 940–942, doi:10.1126/science.1163965.

B. Cai and M. Tan, Key Laboratory of Cenozoic Geology Environment, Institute of Geology and Geophysics, Chinese Academy of Sciences, 19 Beitucheng Xilu, Beijing 100029, China. (cai_bg@mail.iggcas.ac.cn)

X. Jiang and X. Kong, College of Geography Science, Nanjing Normal University, Nanjing 210097, China.

C. Muangsong and N. Pumijumnong, Faculty of Environment and Resource Studies, Mahidol University, Nakhom Pathom 73170, Thailand.

S. Nan, Institute of Climate System, Chinese Academy of Meteorological Sciences, Beijing 100081, China.